Programming Humanoid Motion to Reproduce Human Leg Injuries and Diseases.

Sébastien Lengagne [1], Abderrahmane Kheddar [1,2], Sébastien Druon [1,2] and Eiichi Yoshida [1]

Abstract— In this paper, we present a method of simulating walking motions with leg disease using humanoid robots based on our optimal dynamic multi-contact motion generation technique. We take into account full-body dynamics model of the robot and consider additional physical constraints. We have run the generated motions with HRP-2 humanoid robot platform and identified extra energy consumption due to the constrained leg motions using an infra-red camera. This research is the first step towards the usage of humanoid robots for studies and diagnosis on humans' disabled motions as well as active mannequin for welfare instrument evaluation.

Key Words: humanoid robots, walking, constraints, optimization, disabled motions.

Introduction

In the robotics fields, one usually used biological inspired techniques to reproduce 'natural' motions [1]. However, some methods derived from robotics applications are used to understand and explain human motions and behaviors [2, 3]. In this paper, we apply our previous works on optimal dynamic multi-contact motions generation [4, 5] to reproduce and study leg disease walking motions using the HRP-2 humanoid robot [6].

We aim at studying leg disease walking motions. We cannot used methods based on (over-)reduced models [7, 8, 9] and have to consider a full-body model that takes into account all the physical limits of the robot, the desired contact stances and possibly some additional constraints to reproduce leg diseases (cf. Fig. 1). We generate three walking motions. The first one does not reproduce any disease whereas the second motion simulate the walking motion of someone who sprained its left knee and wear a splint that lock the knee joint position. For the last motion, we consider a broken leg of the robot that, hence, cannot apply important efforts on it. To study the impact of those diseases on the walking motion we use infra-red picture of the robot in order to localize any extra-energy consumption and study the contact forces and knee joint torques obtained from experiments with HRP-2 robot [6].

This work is motivated not only by the enhancement of our optimal motion generation technique, but also by the application of humanoid robots to human study and diagnosis. If we parameterize the disabled motions, we can reproduce different disabled motions to understand and diagnose the cause of the disease. Another application we have in mind is the evaluation of welfare instruments. The proposed method allows the designers of those instruments to evaluate them by simulating various disabled human motions by using the humanoid robot as an "active mannequin".

Section 1. presents the walking motion generation algorithm based on optimization techniques and the additional constraint used to reproduce leg diseases. The experimental results with the HRP-2 robot are presented in Section 2..

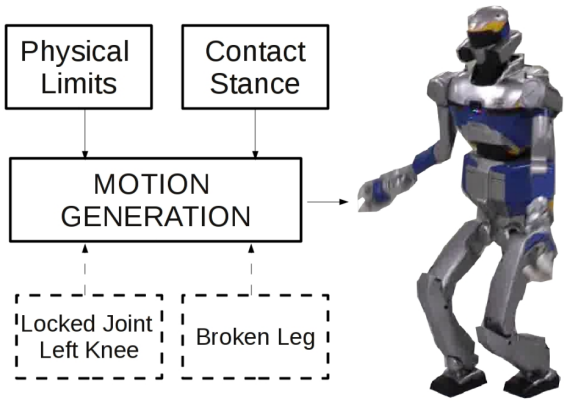

Fig.1 Motion generation software takes into account the physical limits, the desired contact stances and possibly some constraint to reproduce leg disease motions to generate motions performed through HRP-2 Robot.

1. Walking Motion generation

In this Section, we briefly recall the method presented in [4, 5] to generate full-body optimal dynamics multi-contact motion for humanoid robots and virtual avatars and introduce the basics in terms of terminology, notations, and the general formulation of the motion generation problem as an optimization problem.

1·1 Optimization problem

The motion generation problem is equivalent to the optimization one that consists in finding the best set of joint trajectories $q(t)$ that solves:

$$\begin{array}{ll} \underset{q(t)}{\text{argmin}} & C(q(t)) \\ \forall i, \forall t \in [\Delta_i] & g_i(q(t)) \leq 0 \\ \forall j, \forall t \in [\Delta_j] & h_j(q(t)) = 0 \\ \forall t_k \in \{t_1, t_2, \ldots\} & z_k(q(t_k)) \leq 0 \end{array} \quad (1)$$

where C is the cost function to minimize, g is the set of continuous inequality constraints, which usually translates

the physical limits of the system (joint position, velocity, torques, balance, etc.), h is the set of continuous equality constraints, e.g. those which define the position of a link in contact with the environment, z is a set of discrete inequality constraints, e.g. those that can be used to specify the position of one part of the robot at a given time.

As presented in [4, 5], we solve the problem 1, through a B-Spline parametrization of the joint trajectory and a time interval decomposition based on a Taylor polynomials approximation in order to deal with the continuous equality and inequality constraints [10]. Moreover, we compute the contact forces from the joint trajectories and some additional coefficients [4].

1·2 Properties

The walking motions are composed of a cyclic part connected to an initial and final half-sitting posture. Each motion has 9 phases decomposed into 45 intervals. During the experiments, we perform the cyclic part three times. The cost function of this cyclic part is considered more important than the transition parts, during the optimization process. The step size of the walking motion is twenty five centimeters.

It is not easy to guess the cost function that will produce human-like walking. In our case, we consider a weighted sum of the motion duration, square torques and jerks as follows:

$$C = \sum_{i=1}^{N_p} aT_i + \sum_{i=1}^{N_{dof}} \int_0^T \left(b\Gamma_i^2 + c\ddot{q}_i^2 \right) dt \qquad (2)$$

with the weights $a = 5$, $b = 1e^{-2}$, $c = 1e^{-6}$ that are empirically determined through several simulations.

We ensure the feasibility of the motion and the robot's safety by taking into limits about joint position, velocity and torques, unilateral and friction constraints of the contact forces. As discussed in [5], we also consider additional constraints in order to make the motion feasible using the balance controller [11] of the humanoid robot HRP-2 [6]. We generate three different walking motions: one normal walking and two disease leg motions.

1·3 Locked Knee

We study the walking motion as if the robot sprained its knee and wear a splint. We aim at reproducing this walking by artificially lock the left knee joint to a constant value. What we observe from human beings in this situation is the stretched knee by resolving singularity using the additional degrees of freedom (mainly in the hip). As discussed in [5], however, the use of the stabilizer for maintaining balance and the lack of degrees of freedom in legs make stretch knee walking impossible. Therefore, we constraint the left knee joint to 30 degrees.

1·4 Broken Leg

Then, we would like to reproduce walking motions with broken or painful foot. To avoid pain, human beings avoid leaning on the injured foot as much as possible. Thus, we consider an additional constraint on the contact force of the injured left foot. While the ground reaction force is 586N during standby standing posture, we restrain the contact force of the left foot so that it is less than 500N (nearly 85%) during the normal walking motion.

1·5 Optimization process

Table 1 presents the results of the optimization processes to generate the three walking motions.

Table 1 optimization results

walking motion	I	CPU	C
normal	821	3h27mn	166.5
locked knee	510	2h31mn	223.2
broken leg	1427	6h01mn	387.0

Where I, CPU and C represent respectively the number of iterations, the computation time and the final value of the cost function. Obviously, it appears that the normal walking produce the lowest cost functions. Table 1 shows that the walking motion with a broken leg has a bigger cost function than the walking motion with a locked knee. Since the cost function reflects a part of the energy consumption, we can say that the broken leg walking motion is more energy consuming for a humanoid robot, thus should be more tiring for human beings.

2. Experiments

In this section, we present the experimental results we obtain with the HRP-2 robot [6]. The video of those experiments can be found in [12]. Although the motions are a little awkward, we can recognize the disease from those walking motions in the video.

In order to evaluate the energy consumption, we use an infra-red camera (IR-TCM640 from Jenoptik) as presented in Fig. 2 and perform five rounds of the same motion and take an infra-red picture of the legs of the robot which reflects the more significant effects (cf. Figure 2). To get nearly identical thermal conditions, we wait 45 minutes without using the robot between two different walking motions.

2·1 Normal Walking

The normal walking motion is presented in Figure 3. On Figure 2(b), we see that the normal walking does not make excessive energy consumption on any joint. Figures 4 shows the force applied to the legs and emphasizes the fact that the motion is symmetric. The walking motion presented in [12] is not exactly human like even if it is quite smooth, due to the lack of knowledge of the cost function considered by human beings.

2·2 Locked Knee Walking

The locked knee walking motion is presented in Figure 5. The infra-red picture (Fig 2(d)) shows that the right leg (especially the right knee) compensates the disease of the left knee by additional energy consumption. Nevertheless, the right knee joint torques is more important than

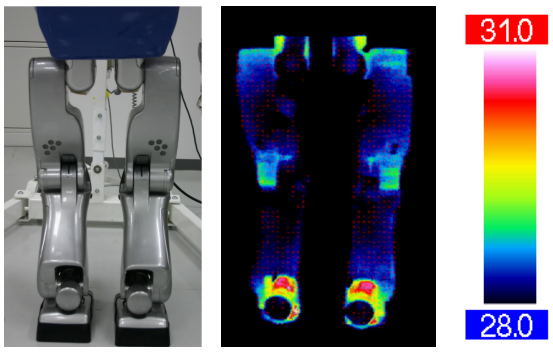

(a) rear view (b) normal walking

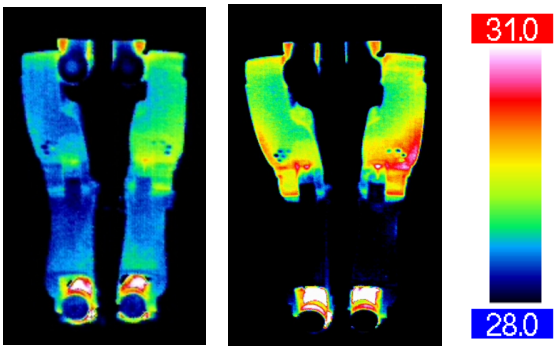

(d) locked knee walking (e) broken leg walking

Fig.2 Infra-red view after five rounds of the walking motions (temperatures are presented in degree Celsius).

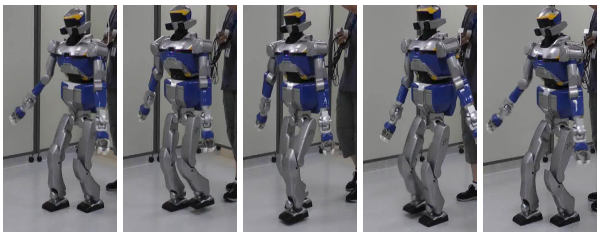

Fig.3 Normal walk without disease reproduction.

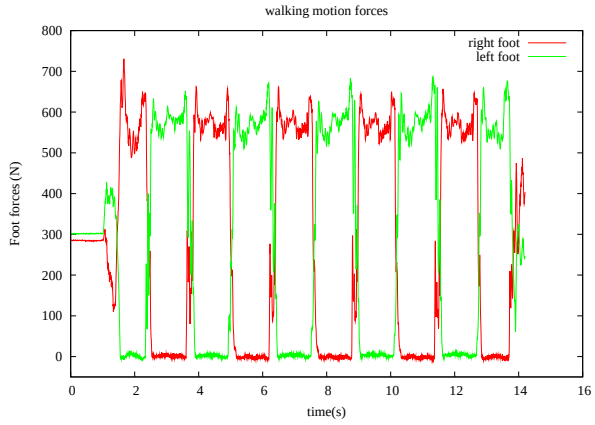

Fig.4 Foot forces during the normal walking

the left one in Figure 6. That explains the larger energy consumption in the right leg.

During the locked knee motion, we did not detect any extra energy consumption in the hip of the robot, whereas for human being this kind of motion leads to fatigue of the hip's muscles. This could be due to a lack of training of the corresponding muscles.

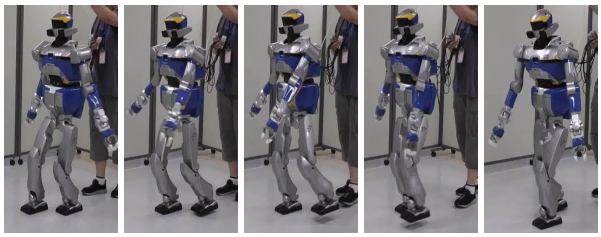

Fig.5 Walking motion with locked knee.

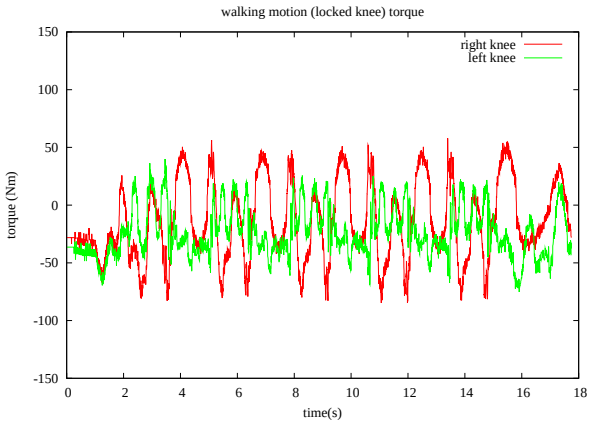

Fig.6 Knee torques during the locked knee walking

2·3 Broken Leg Walking

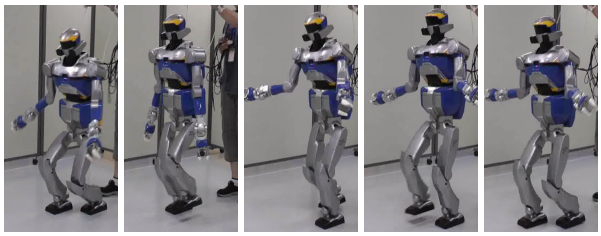

Fig.7 Walking motion with broken leg.

The broken leg walking motion is presented on Figure 7. On Table 1, we see that the cost is more important than for the previous motions, which is also clearly visible on Figure 2(e). We can also observe that the contact forces (cf. Fig. 8) are not symmetric and that the force on the left foot is limited around 500 N except some peaks that may be caused by some unmodeled effects (sharp velocity changes, mechanical flexibilities, ...).

We note the apparition of a preparation phase before the left foot stance phase (during the double support phase) used to accumulate kinetic energy. This preparation was not needed for the previous walking motions and require

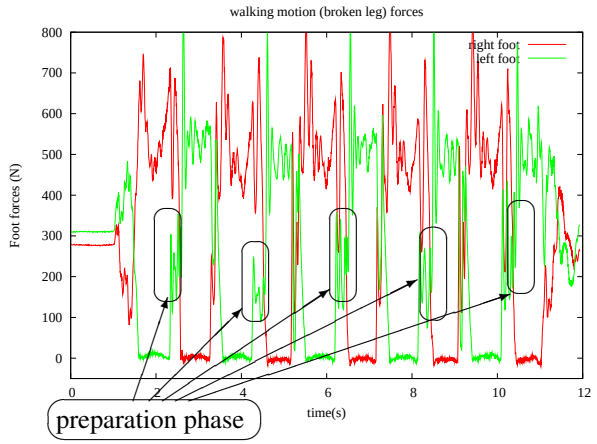

Fig.8 Foot forces during the broken leg walking. The double support phase is used to accumulate kinetic energy to cope the broken leg.

extra energy for both legs in order to cope with the leg disease.

Conclusion

In this paper, we presented a method of reproducing walking motions in case of leg disease by benefiting from our multi-contact motion generation method that can include a variety of constraints on the optimization. The generated motions are experimented with HRP-2 humanoid platform to analyze the energy consumption. We first verified the extra energy consumption is required due to the leg disease using an infra-red camera. We then showed that a locked left knee motion impacts the right leg by making an increase of the right knee torque. It was also demonstrated that the broken leg motions need even larger energy consumption to reduce the ground reaction force, which means avoiding the pain .

In future work, we plan to study how the use of a cane can minimize the effects of leg diseases on the other joint torques and energy consumption using the HRP-2 humanoid robot and virtual human avatars.

[1] A. J. Ijspeert, "Central pattern generators for locomotion control in animals and robots: A review," *Neural Networks*, vol. 21, no. 4, pp. 642–653, may 2008.

[2] M. S. Dutra, A. C. de Pina Filho1and, and V. F. Romano, "Modeling of a bipedal locomotor using coupled nonlinear oscillators of van der pol," *Biological Cybernetics*, vol. 88, no. 4, pp. 286–292, april 2003.

[3] V. Bonnet, P. Fraisse, N. Ramdani, J. Lagarde, S. Ramdani, and B. Bardy, "Modeling Postural Coordination Dynamics using a Closed-Loop Controller," in *8th IEEE-RAS International Conference on Humanoid Robots*, Dec. 2008, pp. 61–66. [Online]. Available: http://hal-lirmm.ccsd.cnrs.fr/lirmm-00345852/en/

[4] S. Lengagne, A. Kheddar, and E. Yoshida, "Generation of optimal dynamic multi-contact motions: Application to humanoid robots." *IEEE Transactions on robotics*, vol. ??, p. ??, 2011, submitted.

[5] ——, "Improving optimization performance for multi-contact motion generation," *Advanced Robotics, special issue Cutting Edge of Robotics in Japan*, 2012, submitted.

[6] K. Kaneko, F. Kanehiro, S. Kajita, H. Hirukawa, T. Kawasaki, M. Hirata, K. Akachi, and T. Isozumi, "Humanoid robot HRP-2," in *IEEE International Conference on Robotics and Automation*, vol. 2, Apr./May 2004, pp. 1083–1090.

[7] S. Kajita, F. Kanehiro, K. Kaneko, K. Fujiwara, K. Yokoi, and H. Hirukawa, "A realtime pattern generator for biped walking," in *IEEE International Conference on Robotics and Automation (ICRA).*, may 2002.

[8] S. Kajita, F. Kanehiro, K. Kaneko, K. Fujiwara, K. Harada, K. Yokoi, and H. Hirukawa, "Biped walking pattern generation by using preview control of zero-moment point," in *IEEE International Conference on Robotics and Automation*, vol. 2, september 2003, pp. 1620 – 1626.

[9] A. Herdt, H. Diedam, P.-B. Wieber, D. Dimitrov, K. Mombaur, and M. Diehl, "Online Walking Motion Generation with Automatic Foot Step Placement," *Advanced Robotics*, vol. 24, pp. 719–737, 2010. [Online]. Available: http://hal.inria.fr/inria-00391408/en/

[10] S. Lengagne, P. Mathieu, A. Kheddar, and E. Yoshida, "Generation of dynamic motions under continuous constraints: Efficient computation using B-Splines and taylor polynomials," in *IEEE/RSJ International Conference on Intelligent Robots and Systems (IROS)*, 2010.

[11] S. Kajita, T. Nagasaki, K. Kaneko, K. Yokoi, and K. Tanie, "A running controller of humanoid biped HRP-2LR," in *IEEE International Conference on Robotics and Automation*, Apr. 2005, pp. 616–622.

[12] [Online]. Available: http://www.youtube.com/watch?v=gx4q23AbWIw